Journal of Biomolecular NMR, **11:** 445–450, 1998.
KLUWER/ESCOM

Heteronuclear correlation experiments for the determination of one-bond coupling constants

Patrik Andersson[a], Kerstin Nordstrand[a], Maria Sunnerhagen[a], Edvards Liepinsh[a], Ivars Turovskis[b] and Gottfried Otting[a,*]
[a]*Department of Medical Biochemistry and Biophysics, Karolinska Institute, S-171 77 Stockholm, Sweden*
[b]*Institute of Organic Synthesis, Aizkraukles iela 21, LV-1006 Riga, Latvia*

Received 10 December 1997; Accepted 15 January 1998

Key words: E. coli arginine repressor, HMQC-α/β, HSQC-α/β, one-bond coupling constants

Abstract

Spin-state selective experiments, HSQC-α/β and CT-HMQC-α/β, are proposed for the simple and rapid measurement of scalar one-bond coupling constants in two-dimensional, ^{1}H-detected ^{15}N-^{1}H or ^{13}C-^{1}H correlation experiments based on HSQC and HMQC schemes. Pairs of subspectra are obtained, containing either the high-field or the low-field component of the doublet representing the one-bond coupling constant. The subspectral editing procedure retains the full sensitivity of HSQC and HMQC spectra recorded without heteronuclear decoupling during data acquisition, with a spectral resolution similar to that of decoupled spectra.

The scalar one-bond coupling constant $^{1}J_{HC}$ of $C^{\alpha}H$ groups is the experimentally most easily accessible parameter with information on the dihedral angle Ψ in proteins and peptides, and it is particularly useful to delineate α-helical secondary structure (Egli and von Philipsborn, 1981a,b; Mierke et al., 1992; Vuister et al., 1992,1993; Edison et al., 1994a,b). $^{1}J_{HC}$ coupling constants are also of interest for the conformational analysis of carbohydrates (Serianni et al., 1995; Church et al., 1997). The dipolar contribution to $^{1}J_{HC}$ and $^{1}J_{HN}$ coupling constants has been shown to contain long-range structural information (Tjandra et al., 1997; Tolman et al., 1997). Methods to measure $^{1}J_{HC}$ coupling constants include 1D ^{13}C spectra recorded without ^{1}H decoupling (Egli and von Philipsborn, 1981a,b), ^{1}H-detected HMQC or 3D HCACO and HCCH-COSY spectra recorded without ^{13}C decoupling during signal detection (Mierke et al., 1992; Vuister et al., 1992), pseudo-3D J-resolved experiments (Vuister et al., 1993) and 2D $^{1}J_{HC}$-modulated CT-HSQC experiments (Tjandra and Bax, 1997). CT-HSQC experiments with and without J-scaling have further been proposed for the precise measurement of $^{1}J_{HN}$ coupling constants (Tolman and Prestegard, 1996a,b). Although the overlap problem in 2D protein NMR spectra recorded without decoupling can be avoided by recording 3D spectra or by encoding the coupling constant in cross-peak intensities, such experiments tend to be more time-consuming than the recording of a simple 2D NMR spectrum. Here we present two-dimensional experiments for the rapid measurement of one-bond coupling constants with high spectral resolution and sensitivity by separating the two doublet components observed in undecoupled HSQC and HMQC spectra into two different subspectra.

Editing the two multiplet components of a doublet into two different subspectra corresponds to separating the resonances for which the coupling partner is in the α or β state. The separation can be achieved by experiments using selective (Nuzillard and Bernassau, 1994; Nuzillard and Freeman, 1994; Fukushi and Kawabata, 1994; Fäcke and Berger, 1996) or exclusively non-selective pulses (Nielsen et al., 1996a,b; Ross et al., 1996; Sattler et al., 1996; Meissner et al., 1997a,b). The scheme proposed here achieves a similar effect as the $S^{3}E$ pulse sequence element of

*To whom correspondence should be addressed.

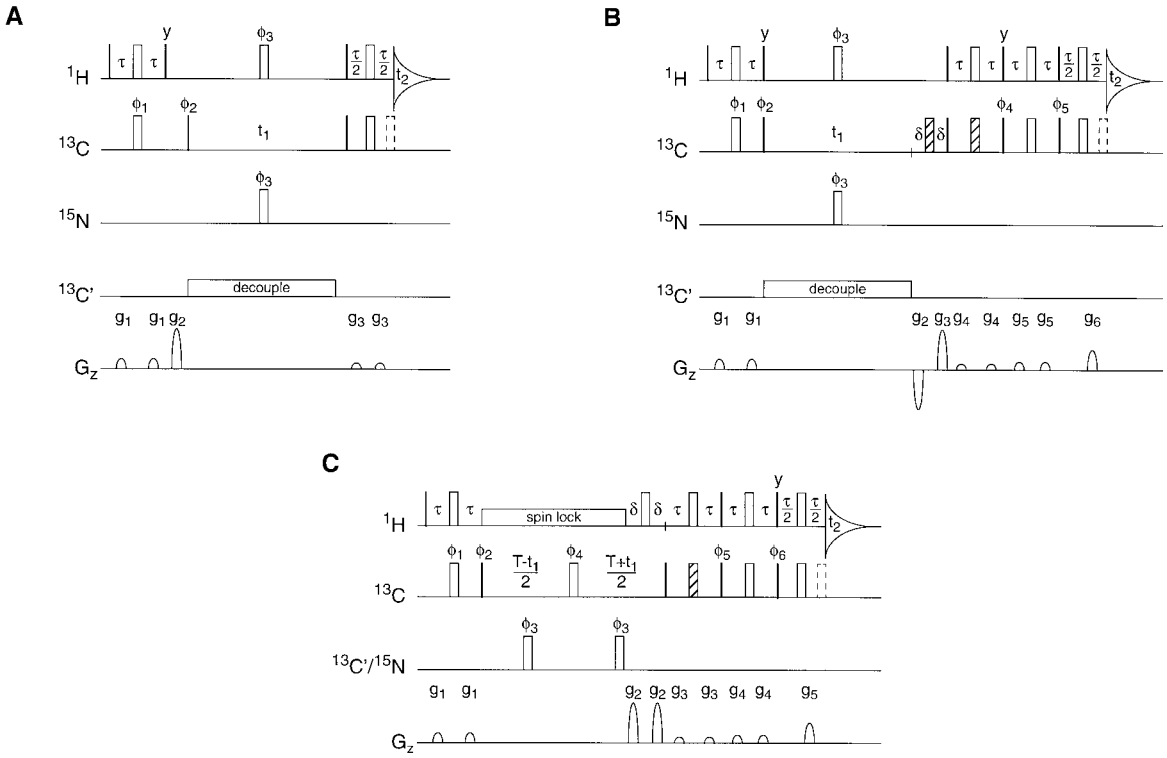

Figure 1. Pulse sequences for the measurement of one-bond scalar couplings. The pulse sequences are exemplified for the measurement of $^1J_{HC}$ coupling constants between α-protons and α-carbons (I = ^{1}H, S = ^{13}C). Narrow (wide) bars represent pulses with flip angles of 90°(180°). Hatched bars denote rectangular 180°(^{13}C) pulses applied at 55 ppm with a duration of 47 μs to avoid excitation of the carbonyl resonances. All pulses, except where noted, are applied with phase x. Two data sets, I and II, are recorded for each experiment which differ by the presence or absence of the editing 180°(^{13}C) pulse (drawn with a dotted line). For optimal subspectral editing, the two data sets should be recorded interleaved, recording the FIDs for each data set before incrementing the evolution time. Before Fourier transformation, the linear combinations I + II and I − II yield two new data sets, IN and AN, containing the in-phase and antiphase peaks. If the FIDs are recorded as complex data points, phase shifting of the data set AN by 90° is easily achieved in the time domain by exchanging the real and imaginary parts of each complex data point in the t_2 dimension and taking the complex conjugate to yield the data set AN_{90}. The linear combinations IN + AN_{90} and IN − AN_{90} can be Fourier transformed as usual to yield the subspectra containing the low-field or high-field doublet components. All pulsed field gradients were applied with a sine-bell shape and a duration of 500 μs and followed by a recovery delay of 300 μs. τ = 1/(4 $^1J_{HC}$) = 1.72 ms, δ = 800 μs. Carbonyl resonances were decoupled either by a 1.0 kHz SEDUCE sequence (McCoy and Mueller, 1992) or by 47 μs 180°(^{13}C) pulses applied at 176 ppm. (A) Pulse sequence of the HSQC-α/β experiment. Phase cycle: ϕ_1 = x; ϕ_2 = x,−x; ϕ_3 = 2(x),2(−x); receiver = x,−x. Gradient strengths: $g_{1,2,3}$ = 2.5, 10.0, 2.0 G/cm. (B) Sensitivity-enhanced HSQC-α/β experiment. Phase cycle: ϕ_1 = x; ϕ_2 = x,−x; ϕ_3 = 2(x),2(−x); ϕ_4 = y; ϕ_5 = 4(x),4(−x); receiver = x,−x. Gradient strengths: $g_{1,2,3,4,5,6}$ = 2.5, −9.9, 9.9, 1.5, 2.0, 5.0 G/cm. For phase-sensitive spectra and quadrature detection in the indirect frequency dimension, the sign of the gradients g_2 and g_3 is inverted together with the pulse phase ϕ_4 and the resulting echo-/antiecho data stored separately (Kay et al., 1992). (C) Sensitivity-enhanced constant-time HMQC-α/β experiment. T = 28 ms. Phase cycle: $\phi_1 = \phi_2$ = x; ϕ_3 = 8(x),8(−x); ϕ_4 = x,y,−x,−y; ϕ_5 = −y; ϕ_6 = 4(x),4(−x); receiver = x,−x. Gradient strengths: $g_{1,2,3,4,5}$ = 2.5, 9.9, 1.5, 2.0, 5.0 G/cm. Echo-/antiecho data are recorded by sign alternation of the gradient g_2 with simultaneous inversion of phase ϕ_5 (Kay et al., 1992). The ^{1}H spin-lock power was 6.25 kHz. In (A), axial peaks are shifted to the side of the spectrum by incrementing the phases ϕ_1 and ϕ_2 by 90° together with the time incrementation of the evolution time t_1. In (B) and (C), axial peak artifacts are shifted to the side of the spectrum by inverting the phases ϕ_1 and ϕ_2 together with the receiver phase for the FIDs recorded for every other evolution time increment.

Sørensen and co-workers (Meissner et al., 1997a,b; Sørensen et al., 1997), but is simpler to combine with sensitivity enhancement and water flip-back schemes when measuring $^1J_{HC}$ or $^1J_{HN}$ coupling constants from HSQC- or HMQC-type spectra.

In terms of Cartesian product operators (Sørensen et al., 1983), single multiplet components can be described as the sum or difference of in-phase and antiphase magnetization, $I_x \pm 2I_xS_z$. Starting from in-phase magnetization I_x, evolution under the scalar coupling J with the spin S generates antiphase magnetization $2I_yS_z$, i.e. magnetization with a phase orthogonal with respect to the starting magnetization. Equal amounts of in-phase and antiphase magnetization are

present after a coupling evolution period of 1/(4J). Application of a 180°(S) pulse inverts the sign of the antiphase but not the in-phase magnetization. Thus, recording two experiments with and without a 180°(S) pulse yields two data sets which, after addition and subtraction, contain pure in-phase and antiphase magnetization, respectively. Subsequently, the data set representing the $2I_yS_z$ magnetization can be phase corrected by 90°, corresponding to a conversion of $2I_yS_z$ to $2I_xS_z$. At this stage, the subspectra containing the in-phase and antiphase multiplets can be combined by addition or subtraction to yield spectra with one or the other multiplet component. The scheme is closely related to the half-filter element (Otting et al., 1986), except that the delay is 1/(4J) instead of 1/(2J) and for the additional data processing.

Figure 1 shows implementations of this 'α/β-half-filter' scheme in HSQC, sensitivity-enhanced HSQC (SE-HSQC) and sensitivity-enhanced HMQC (SE-HMQC) experiments. The HSQC-α/β experiment (Figure 1A) differs from the original HSQC experiment (Bodenhausen and Ruben, 1980) by the shorter delay of the refocusing INEPT step, during which antiphase magnetization $2I_yS_z$ present after the last 90°(I) pulse refocuses into equal amounts of antiphase and in-phase magnetization, and the fact that two experiments must be recorded which differ by the presence or absence of a 180°(S) pulse before signal detection. Optional pulsed field gradients (PFG) support the selection of the desired coherence transfer pathway. Similarly, optional decoupling pulses were implemented in the experimental scheme of Figure 1A for improved performance with $^1J_{HC}$ measurements of $C^\alpha H$ groups ($I = {}^1H$, $S = {}^{13}C$).

Figure 1B shows the pulse sequence of a sensitivity-enhanced HSQC experiment (Palmer III et al., 1991; Kay et al., 1992) with PFGs for coherence selection. Phase-modulated in-phase magnetization is present after the last 90°(I) pulse, which defocuses during the following spin-echo period $\tau = 1/(4J)$ into equal amounts of in-phase and antiphase magnetization. Two data sets are recorded which differ by the presence or absence of the editing 180°(S) pulse before signal detection. The last 90°(S) pulse is not necessary for coherence transfer, but was experimentally found to reduce cross-talk between the subspectra.

Figure 1C shows the pulse sequence of a constant-time HMQC experiment (Grzesiek and Bax, 1995) with coherence selection by PFGs and sensitivity-enhancement. Phase-modulated in-phase magnetization is present after the last 90°(I) pulse, which defocuses during the following spin-echo period into equal amounts of in-phase and antiphase magnetization. Two data sets must be recorded which differ by the presence or absence of the editing 180°(S) pulse before signal detection, in complete analogy to the SE-HSQC experiment of Figure 1B.

Spectra using the pulse sequences of Figure 1 were recorded with a 30% ^{13}C/100%^{15}N labelled sample of the 78-residue amino terminal domain of the *E. coli* arginine repressor (Sunnerhagen et al., 1997) dissolved in D_2O. Figure 2A–C shows the spectral region containing the ^{13}C-^1H cross peaks of the $C^\alpha H$ resonances in the subspectra containing the low-field doublet component from HSQC-α/β, SE-HSQC-α/β and SE-CT-HMQC-α/β experiments, respectively. Cross sections through the cross peak of Phe^{14} are shown in Figure 2 for all pairs of subspectra of the respective experiments, illustrating the separation of the doublet components into different subspectra. As expected, the signal-to-noise ratio of the HSQC-α/β experiment (Figure 2A) is achieved in a shorter time using the sensitivity-enhanced HSQC-α/β experiment (Figure 2B). The suppression of the high-field (low-field) doublet component in the subspectra selecting the low-field (high-field) component depends on the delay τ and the magnitude of the coupling constants. Amino acid residues with $^1J_{HC}$ couplings larger (smaller) than 4τ yield too much (little) antiphase magnetization and therefore imperfect peak selection. Since the $^1J_{HC}$ coupling constants of $C^\alpha H$ groups do not vary much between different residues, the suppression of the undesired multiplet component was generally very good. If necessary, complete suppression of the undesired multiplet component can be achieved for selected cross peaks by combining the data sets containing the in-phase and antiphase multiplets with different weights. Small up-field shifts of the cross peaks in Figures 2A and B in the ^{13}C-dimension are from off-resonant effects from the SEDUCE decoupling used (Figure 1; McCoy and Mueller, 1992). The $^1J_{HC}$ values measured for the N-terminal arginine repressor domain were in good agreement with the Ψ angles observed in the NMR structure (Figure 3; Sunnerhagen et al., 1997). Measurements from the HSQC-α/β and sensitivity-enhanced constant-time HMQC-α/β experiments correlated with an rms deviation of 0.9 Hz.

The pulse sequences presented here are of similar duration as the standard sequences they were derived from, which is advantageous for proteins with short relaxation times. More specifically, the pulse sequence

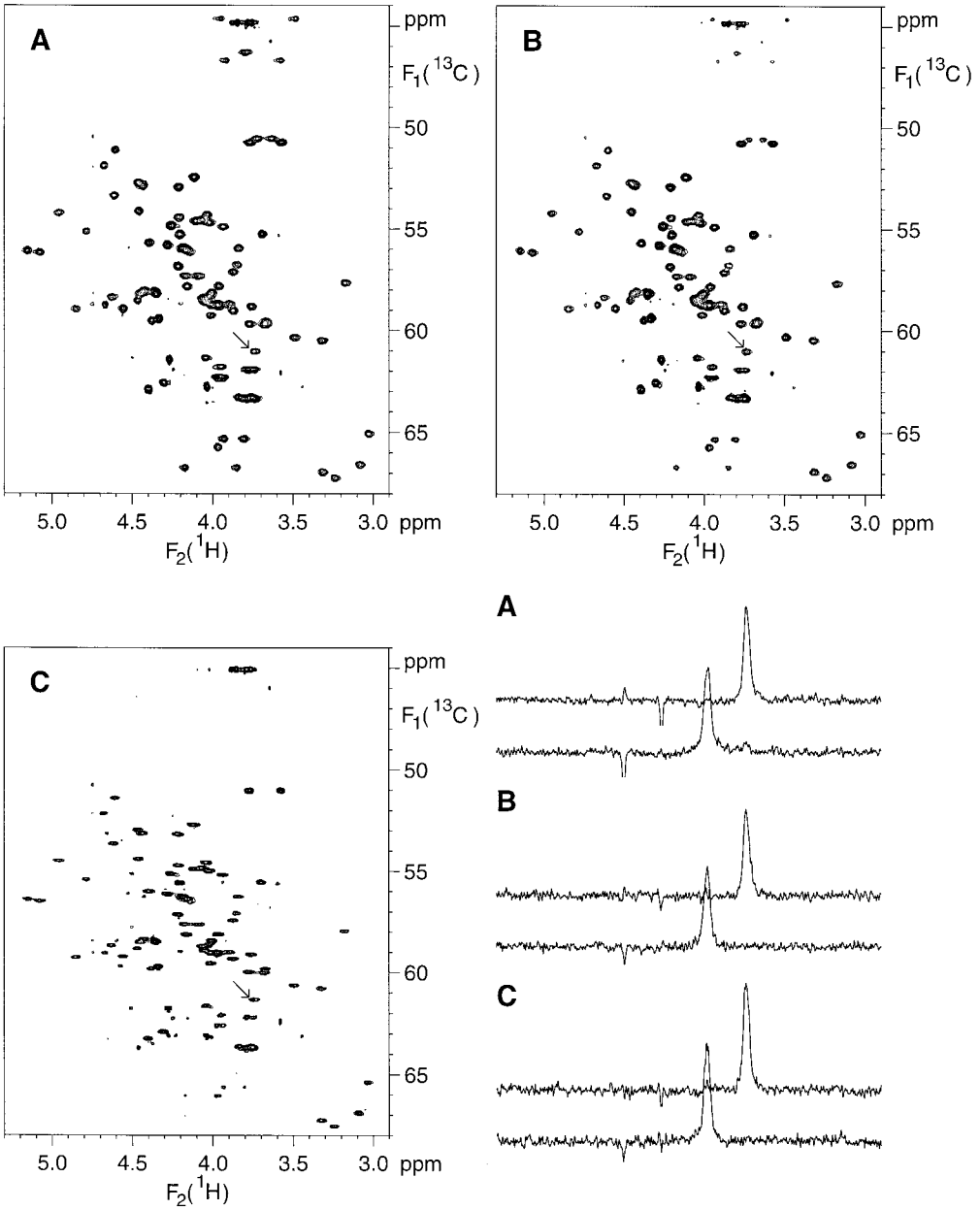

Figure 2. HSQC-α/β (A), sensitivity-enhanced HSQC-α/β (B) and sensitivity-enhanced CT-HMQC-α/β (C) spectra recorded with a 3 mM solution of the 30% ^{13}C/100% ^{15}N-labelled 78 residue N-terminal domain of the *E. coli* arginine repressor at 28 °C, pH 5.5, using the pulse sequences of Figure 1. The 2D spectra display only the spectral region containing the $^{13}C^{\alpha}$-$^{1}H^{\alpha}$ cross peaks from the subspectra containing the low-field doublet component. One-dimensional cross sections through the cross peak of Phe[14] (identified by an arrow) are shown for the pairs of subspectra of each experiment. All data were recorded on a Bruker DMX-600 NMR spectrometer using $t_{2max} = 341$ ms. Before Fourier transformation, the data were multiplied by a cosine squared window function in the t_2 dimension and a sine-bell window shifted by $\pi/4$ in the t_1 dimension, except that a cosine window function was used in the t_1 dimension of the CT-HMQC-α/β experiment after 1.8-fold extension by linear prediction. The HSQC-α/β, sensitivity-enhanced HSQC-α/β and sensitivity-enhanced CT-HMQC-α/β experiments were recorded with total experimental times of 6 h, 4 h and 4.5 h, using 24, 16 and 32 transients per t_1 value and t_{1max} of 50 ms, 50 ms and 27 ms, respectively. The protein sample was expressed and purified as described (Sunnerhagen et al., 1997), but M9 minimal medium containing 4.5 g/l 30% ^{13}C/100% ^{15}N-labelled algal extract as the carbon source was used. The algal extract was produced after the procedure of Sørensen and Poulsen (1992).

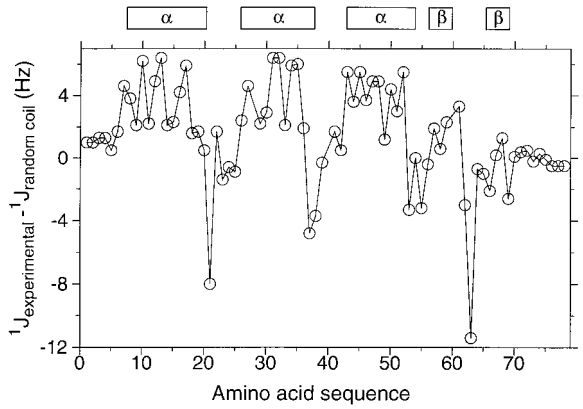

Figure 3. Difference between the $^1J_{HC}$ coupling constants of $C^{\alpha}H$ groups measured for the N-terminal domain of the *E. coli* arginine repressor and random coil values by Vuister et al. (1993). The regular secondary structure elements identified by the NMR structure of the protein (Sunnerhagen et al., 1997) are indicated at the top.

of Figure 1A is shorter than that of an HSQC experiment with a refocusing INEPT step before signal detection (Bodenhausen and Ruben, 1980), while the experiments of Figures 1B and C employ gradient refocusing delays of $\tau/2$, which is not much longer than the delays normally used in gradient-enhanced schemes (Kay et al., 1992; Schleucher et al., 1994). Furthermore, the editing 180°(S) pulse before signal detection is the only additional pulse required, minimizing adverse effects from pulse imperfections. The experiments are as sensitive as the HSQC and HMQC experiments they were derived from. They are thus particularly attractive for measurements at natural isotope abundance. Partial ^{13}C enrichment at a level of 30% is advantageous to narrow the cross peaks in the F1 frequency dimension of Figures 2A and B, while the constant-time experiment of Figure 1C is designed to remove J_{CC} couplings otherwise observed with 100% isotope enriched samples. The experiments can be used to measure $^1J_{HC}$ couplings for CH_2 and CH_3 groups as well as for CH groups, except that the delays of the sensitivity-enhancement scheme in Figures 1B and C would have to be readjusted (Schleucher et al., 1992). The experiments yield not only one-bond coupling constants from the doublet peak separation, but also information about dipole–dipole and dipole–CSA cross correlation from the different linewidths observed for the high-field and low-field doublet components (Goldman, 1984; Čuperlović et al., 1996; Tolman and Prestegard, 1996a; Tjandra and Bax, 1997; Pervushin et al., 1997).

Acknowledgements

P.A. acknowledges an SSF fellowship within the Strategic Research in Structural Biology programme. Financial support from the Swedish Natural Science Research Council (project 10161) is gratefully acknowledged.

References

Bodenhausen, G. and Ruben, D.J. (1980) *Chem. Phys. Lett.*, **69**, 185–189.
Church, T.J., Carmichael, I. and Serianni, A.S. (1997) *J. Am. Chem. Soc.*, **119**, 8946–8964.
Čuperlović, M., Palke, W.E., Gerig, J.T. and Gray, G.A. (1996) *J. Magn. Reson.*, **B110**, 26–38.
Edison, A.S., Markley, J.L. and Weinhold, F. (1994a) *J. Biomol. NMR*, **4**, 519–542.
Edison, A.S., Weinhold, F., Westler, W.M. and Markley, J.L. (1994b) *J. Biomol. NMR*, **4**, 543–551.
Egli, H. and von Philipsborn, W. (1981a) *Helv. Chim. Acta*, **64**, 976–988.
Egli, H. and von Philipsborn, W. (1981b) *Org. Magn. Reson.*, **15**, 404–406.
Fäcke, T. and Berger, S. (1996) *J. Magn. Reson.*, **A119**, 260–263.
Fukushi, E. and Kawabata, J. (1994) J. Magn. Reson., **A108**, 103–105.
Goldman, M. (1984) *J. Magn. Reson.*, **60**, 437–452.
Grzesiek, S. and Bax, A. (1995) *J. Biomol. NMR*, **6**, 335–339.
Kay, L.E., Keifer, P. and Saarinen, T. (1992) *J. Am. Chem. Soc.*, **114**, 10663–10665.
McCoy, M.A. and Mueller, L. (1992) *J. Magn. Reson.*, **99**, 18–36.
Meissner, A., Duus, J.Ø. and Sørensen, O.W. (1997a) *J. Magn. Reson.*, **128**, 92–97.
Meissner, A., Duus, J.Ø. and Sørensen, O.W. (1997b) *J. Biomol. NMR*, **10**, 89–94.
Mierke, D.F., Grdadolnik, S.G. and Kessler, H. (1992) *J. Am. Chem. Soc.*, **114**, 8283–8284.

Nielsen, N.C., Thøgersen, H. and Sørensen, O.W. (1996a) *J. Chem. Phys.*, **105**, 3962–3968.
Nielsen, N.C., Thøgersen, H. and Sørensen, O.W. (1996b) *J. Am. Chem. Soc.*, **117**, 11365–11366.
Nuzillard, J.-M. and Bernassau, J.-M. (1994) *J. Magn. Reson.*, **B103**, 284–287.
Nuzillard, J.-M. and Freeman, R. (1994) *J. Magn. Reson.*, **A110**, 262–265.
Otting, G., Senn, H., Wagner, G. and Wüthrich, K. (1986) *J. Magn. Reson.*, **70**, 500–505.
Palmer III, A.G., Cavanagh, J., Wright, P. and Rance, M. (1991) *J. Magn. Reson.*, **93**, 151–170.
Pervushin, K., Riek, R., Wider, G. and Wüthrich, K. (1997) *Proc. Natl. Acad. Sci. USA*, **94**, 12366–12371.
Ross, A., Czisch, M. and Holak, T.A. (1996) *J. Magn. Reson.*, **A118**, 221–226.
Sattler, M., Schleucher, J., Schedletzky, O., Glaser, S.J., Griesinger, C., Nielsen, N.C. and Sørensen, O.W. (1996) *J. Magn. Reson.*, **A119**, 171–179.
Schleucher, J., Schwendinger, M., Sattler, M., Schmidt, P., Schedletzky, O., Glaser, S.J., Sørensen, O.W. and Griesinger, C. (1994) *J. Biomol. NMR*, **4**, 301–306.
Serianni, A.S., Wu, J. and Carmichael, I. (1995) *J. Am. Chem. Soc.*, **117**, 8645–8650.
Sørensen, M.D., Meissner, A. and Sørensen, O.W. (1997) *J. Biomol. NMR*, **10**, 181–186.
Sørensen, O.W., Eich, G.W., Levitt, M.H., Bodenhausen, G. and Ernst, R.R. (1983) *Prog. NMR Spectrosc.*, **16**, 163–192.
Sørensen, P. and Poulsen, F.M. (1992) *J. Biomol. NMR*, **2**, 99–101.
Sunnerhagen, M., Nilges, M., Otting, G. and Carey, J. (1997) *Nat. Struct. Biol.*, **4**, 819–826.
Tjandra, N. and Bax, A. (1997) *J. Magn. Reson.*, **124**, 512–515.
Tjandra, N., Omichinski, J.G., Gronenborn, A.M., Clore, G.M. and Bax, A. (1997) *Nat. Struct. Biol.*, **4**, 732–738.
Tolman, J.R. and Prestegard, J.H. (1996a) *J. Magn. Reson.*, **B112**, 245–252.
Tolman, J.R. and Prestegard, J.H. (1996b) *J. Magn. Reson.*, **B112**, 269–274.
Tolman, J.R., Flanagan, J.M., Kennedy, M.A. and Prestegard, J.H. (1997) *Nat. Struct. Biol.*, **4**, 292–297.
Vuister, G.W., Delaglio, F. and Bax, A. (1992) *J. Am. Chem. Soc.*, **114**, 9674–9675.
Vuister, G.W., Delaglio, F. and Bax, A. (1993) *J. Biomol. NMR*, **3**, 67–80.